JTL 14 (2) DECEMBER 2025
Page: 322-334

Contents list available at Jurnal Teknologi Laboratorium

JURNAL TEKNOLOGI LABORATORIUM

Journal Homepage: www.teknolabjournal.com
ISSN 2580-0191(Online) I ISSN 2338 – 5634(Print)

Original Research

Effects of EH-MSC–derived exosomes on oxidative stress and inflammatory markers in a UVB-induced skin damage rat model

Meri [1], Agung Putra [2,3,4], Chodijah [5], Eko Setiawan [1,6]

[1] Department of Postgraduate Biomedical Science, Faculty of Medicine, Sultan Agung Islamic University, Semarang, Indonesia
[2] Stem Cell and Cancer Research (SCCR) Laboratory, Faculty of Medicine, Sultan Agung Islamic University, Semarang, Indonesia
[3] Department of Pathological Anatomy, Faculty of Medicine, Sultan Agung Islamic University, Semarang, Indonesia
[4] Department of Doctoral Biomedical Science, Faculty of Medicine, Sultan Agung Islamic University, Semarang, Indonesia
[5] Department of Anatomy, Faculty of Medicine, Sultan Agung Islamic University, Semarang, Indonesia
[6] Department of Surgery, Faculty of Medicine, Sultan Agung Islamic University, Semarang, Indonesia

Abstract: Prolonged exposure to ultraviolet B (UVB) radiation causes persistent skin inflammation, resulting in oxidative stress, collagen breakdown, and progressive loss of collagen. Exosomes generated from mesenchymal stem cells of the umbilical cord (EH-MSCs) have surfaced as a promising cell-free therapeutic approach owing to their anti-inflammatory and antioxidant characteristics. This experimental work assessed the impact of EH-MSC exosomes on inflammatory and oxidative stress indicators in a rat model of collagen loss induced by UVB exposure. Wistar rats were categorized into five groups: healthy control (G1), UVB-exposed animals administered NaCl (G2), hyaluronic acid (G3), 200 µL of EH-MSC exosomes (G4), and 300 µL of EH-MSC exosomes (G5). Exosomes were extracted from rat umbilical cord mesenchymal stem cells via tangential flow filtration and subsequently analyzed using flow cytometry. Tumor necrosis factor-alpha (TNF-α) and glutathione peroxidase (GPx) concentrations were quantified via ELISA, and statistical evaluation was conducted employing ANOVA and Kruskal–Wallis tests. The minimal TNF-α levels were recorded in the healthy control group (72.08 ± 18.30 pg/mL), whereas the maximal values were identified in the hyaluronic acid group (216.80 ± 56.27 pg/mL). Subcutaneous delivery of EH-MSC exosomes in G4 and G5 markedly decreased TNF-α levels in comparison to the saline and hyaluronic acid groups ($p < 0.05$). GPx levels were maximal in the G5 group (722.60 ± 57.67 pg/mL) and minimal in the saline-treated group (46.90 ± 11.29 pg/mL). Marked disparities in GPx levels were noted among the treatment groups ($p < 0.05$). The results demonstrate that subcutaneous delivery of EH-MSC exosomes at dosages of 200 µL and 300 µL significantly reduces inflammation and improves antioxidant activity in UVB-induced collagen degradation. EH-MSC exosomes exhibit promise as a cell-free therapeutic strategy for alleviating UVB-induced skin damage.

Keywords: Collagen Loss; EH-MSC; GPx; TNF alpha.

INTRODUCTION

Ultraviolet B (UV-B) radiation is a major environmental factor that accelerates skin aging by triggering oxidative stress and inflammation, ultimately

Corresponding author.
E-mail address: merilfc81@gmail.com (Meri)
DOI: 10.29238/teknolabjournal.v14i2.575
Received 27 January 2025; Received in revised form 13 September 2025; Accepted 07 November 2025

leading to collagen degradation and loss of skin elasticity [1]. The imbalance caused by excessive reactive oxygen species (ROS) overwhelms the skin's antioxidant defenses, particularly Glutathione Peroxidase (GPx), a key enzyme in mitigating oxidative damage. Simultaneously, UV-B-induced ROS activates inflammatory pathways, leading to overexpression of Tumor Necrosis Factor Alpha (TNF-α), a pro-inflammatory cytokine associated with skin damage and collagen breakdown. [2,3] These mechanisms contribute to photoaging and highlight the critical need for therapies that address both oxidative stress and inflammation.

Current interventions, such as hyaluronic acid (HA)-based treatments, primarily focus on hydration and structural support for the extracellular matrix [4]. However, they fall short in directly addressing the root causes of oxidative stress and inflammation.[5,6] Consequently, these therapies provide only temporary benefits, leaving untreated the chronic inflammatory and oxidative pathways that lead to relapse. [6]

Recent research has identified mesenchymal stem cell-derived exosomes, particularly those derived under hypoxic conditions (EH-MSC), as a promising therapeutic strategy. Exosomes are nanovesicles rich in bioactive molecules such as microRNAs (e.g., miR-146a, miR-21) and anti-inflammatory cytokines like interleukin-10 (IL-10). [7–11] These components have been shown to suppress TNF-α expression, modulate the NF-κB signaling pathway, and enhance antioxidant defenses through GPx upregulation. [12] Although in vitro studies have demonstrated their efficacy in skin rejuvenation and mitigating oxidative stress, limited in vivo research exists that directly evaluates the effects of EH-MSC exosomes on TNF-α and GPx levels under UV-B-induced conditions. [13]

Previous studies have predominantly focused on the regenerative effects of exosomes from diverse MSC sources. For instance, Gao et al. (2021) demonstrated that adipose-derived MSC exosomes activate the TGF-β/Smad pathway to enhance collagen synthesis in UV-B-exposed fibroblasts. [13,14] Similarly, Yan et al. (2023) reported that bone marrow-derived MSC exosomes containing miR-29b-3p alleviate UV-induced photoaging through MMP suppression.[15] While these findings underline the potential of MSC exosomes, they are limited to in vitro settings and primarily explore pathways unrelated to TNF-α or GPx modulation. Moreover, studies utilizing amnion-derived exosomes have focused on DNA repair and inflammation reduction but lack specificity in addressing oxidative stress markers like GPx.[16]

The novelty of this research lies in its focus on EH-MSC-derived exosomes demonstrates superior antioxidant and anti-inflammatory with modulation of TNF-α and GPx in an in vivo model of UV-B-induced damage.[17–19] By targeting these two critical biomarkers, this study aims to bridge the gap between exosome-based therapies and their application in managing the underlying mechanisms of photoaging. Unlike previous research, this study leverages the unique properties of hypoxia-conditioned MSC exosomes, known for their enhanced bioactive molecule content, to provide a more effective therapeutic approach to oxidative and inflammatory skin damage.

The primary objective of this study is to evaluate the effects of subcutaneous EH-MSC exosome injections on reducing TNF-α levels and enhancing GPx activity in UV-B-exposed models. This research posits that EH-MSC exosomes, through their enriched anti-inflammatory and antioxidant properties, can simultaneously counteract oxidative stress and inflammation, offering a novel intervention for UV-B-induced skin damage.

MATERIAL AND METHOD

Study Design

This research utilized an in vivo experimental design to investigate the effects of subcutaneous EH-MSC exosome injections on oxidative stress and inflammation in Wistar rats exposed to UV-B radiation. The study followed a

Randomized Post-Test Only Control Group Design, consisting of five groups: a control group (G1) and four treatment groups (G2-G5). G2 received NaCl injections, G3 received hyaluronic acid (HA), while G4 and G5 received EH-MSC exosomes at 200 µL and 300 µL. This experimental setup enabled precise comparison between treated and untreated groups while minimizing potential bias.

The research was conducted at the Laboratory of Stem Cell and Cancer Research (SCCR), Semarang, Indonesia, between April and May 2024. Histological and ELISA analyses were completed within the same facility.

Ethical Clearance

The study was approved by the Ethics Committee of the Faculty of Medicine, Sultan Agung Islamic University, with reference number No.133/IV/202/Komisi Bioetik.

Exosome Cultivation and Isolation

Mesenchymal stem cells (MSCs) were isolated from the umbilical cords of 21-day pregnant rats and cultured under optimized conditions to ensure sufficient exosome production. The cells were grown in Dulbecco's Modified Eagle Medium (DMEM, high-glucose, Gibco, USA), supplemented with 10% heat-inactivated fetal bovine serum (FBS, Gibco, USA) and 1% penicillin-streptomycin (Gibco, USA)[20,21]. MSCs were passaged five times to expand the cell population, with spindle-shaped cells characteristic of MSC morphology observed under a microscope[20]. To enhance exosome production, the MSCs were incubated under hypoxic conditions (5% oxygen concentration) for 24 hours in a hypoxia chamber[22]. These conditions stimulated the secretion of exosomes enriched with bioactive molecules such as miR-21 and miR-146a, essential for antioxidant and anti-inflammatory responses. The conditioned culture media containing secretomes, including exosomes, were collected into sterile bottles and temporarily stored at 4°C[23].

Exosomes were isolated from the conditioned media using the uPulse Tangential Flow Filtration (TFF) system (Millipore, Germany). The media were filtered through molecular weight cut-off filters of 100 kDa and 500 kDa to remove larger particles while concentrating the exosome fraction. The filtrate was further processed to maximize exosome yield. The isolated exosomes were validated for quality and purity using flow cytometry to detect characteristic exosomal surface markers, including CD9, CD63, and CD81. The validated exosomes were aliquoted into 2.5 mL sterile tubes and stored at 2–8°C for short-term use or −80°C for long-term storage to ensure stability and functionality.

Animal Model

Male Wistar rats aged 6–8 weeks, weighing 225 ± 22.5 grams, were used as the experimental model. Inclusion criteria required the rats to be healthy and without anatomical abnormalities, while rats with illness, deformities, or prior participation in studies were excluded. A total of 30 rats were randomly assigned into five groups. After a seven-day acclimatization period under standard laboratory conditions (20–25°C, ad libitum access to food and water), the rats were exposed to UV-B radiation to induce collagen loss.

UV-B Exposure

The dorsal area of the rats was shaved (2 × 3 cm) under anesthesia (ketamine 99%, 60 mg/kg BW, and xylazine 98%, 20 mg/kg BW) before UV-B radiation exposure. A UV-B lamp delivered a dose of 150 mJ/cm² at a fixed distance of 20 cm. Each session lasted for 8 minutes and was conducted five times weekly for two consecutive weeks. This procedure was standardized to induce consistent collagen loss across the experimental groups[24].

Treatment Protocol

Injections were administered on days 1 and 7 following UV-B exposure across five experimental groups. The first group (G1) served as the control group and did not receive UV-B exposure or any treatment. The second group (G2) was treated with a subcutaneous injection of 200 µL saline (NaCl 0.9%, Merck, Germany). The third group (G3) received a subcutaneous injection of 200 µL

hyaluronic acid (Sigma-Aldrich, USA). The fourth group (G4) was injected subcutaneously with 200 µL of EH-MSC exosomes, while the fifth group (G5) received 300 µL of EH-MSC exosomes via subcutaneous injection[25].

Validation of Collagen Loss

Validation of collagen loss was conducted to confirm the skin damage induced by UV-B exposure. Macroscopic assessment involved observing the skin for visible damage such as wrinkling and redness in the UV-B-exposed groups. Histological validation was performed using Masson's Trichrome staining to evaluate collagen degradation. Tissue sections were examined under an Olympus BX53 microscope to assess structural changes caused by UV-B exposure and to observe collagen fibers[26,27].

Sample Collection

On day 15, skin samples were collected from the dorsal area of the rats and homogenized in RIPA buffer (Thermo Fisher Scientific, USA). The homogenized samples were stored at −80°C until further analysis. Care was taken to ensure equal representation of samples across all experimental groups to maintain consistency in the analysis[28].

Biochemical Analysis (ELISA)

Biochemical analysis of TNF-α and GPx levels was performed using ELISA kits (Elabscience, USA). The ELISA procedure included adding skin homogenates to wells coated with specific antibodies, followed by incubation with primary and secondary antibodies conjugated to enzymes. A chromogenic substrate was introduced to initiate a colorimetric reaction, and absorbance was measured at 450 nm using the Shimadzu UV-1900 spectrophotometer. Each sample was processed in triplicate to ensure the reliability and accuracy of the results[29].

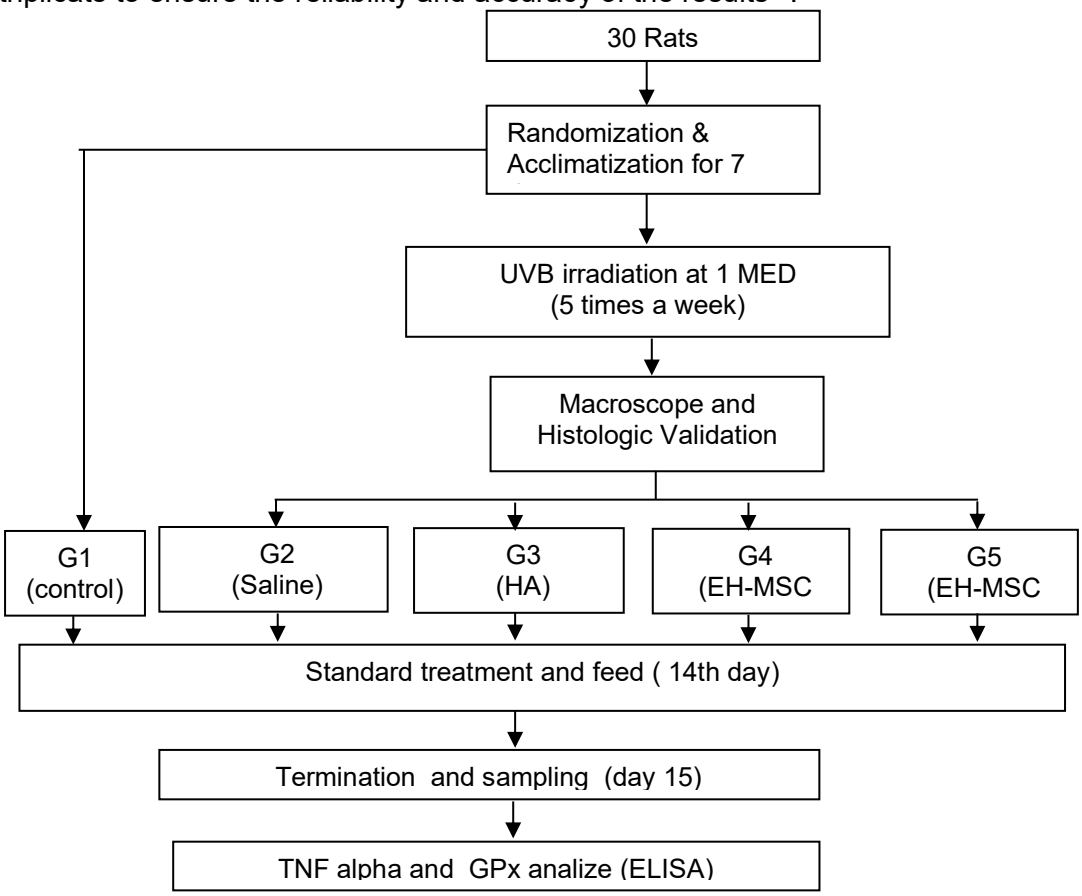

Figure 1. Design Study

Data Analysis

Data were analyzed using SPSS (version 26.0; Document number: 869358; IBM Corp., Armonk, NY)[30]. Normality was tested using the Shapiro-Wilk test, and homogeneity was assessed with Levene's test. Parametric data were analyzed using one-way ANOVA, followed by Post Hoc LSD or Tamhane's tests depending on homogeneity. Non-parametric data were analyzed using the Kruskal-Wallis test, with pairwise comparisons via Mann-Whitney tests. Statistical significance was set at $p < 0.05$.

RESULTS AND DISCUSSION

Research Results

Validation of EH-MSC

The isolation of mesenchymal stem cells (MSCs) was conducted using the umbilical cords of 21-day pregnant rats. The isolated cells were cultured in a specialized flask using specific culture media. The fifth passage of MSC cultures showed spindle-like adherent cells when observed under a microscope (Figure 2A).

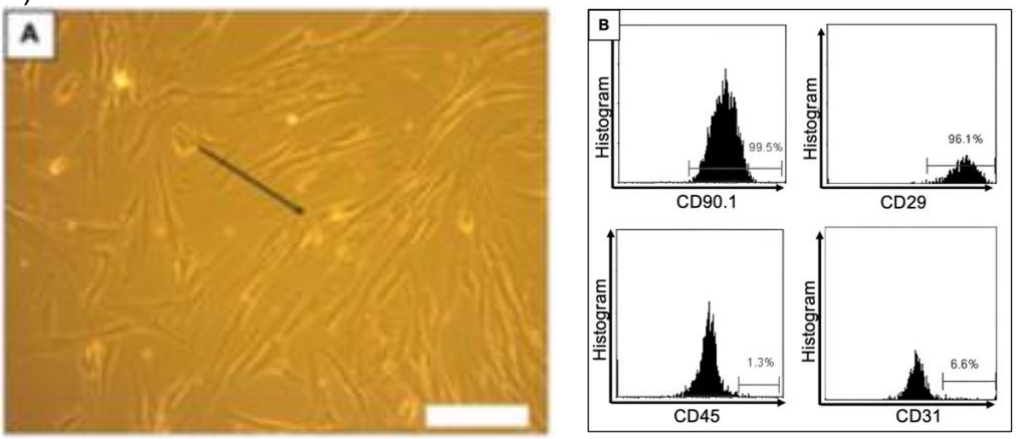

Figure 2. (A) MSC isolation at 80% confluence shows spindle-like cell morphology (indicated by arrows) at 100x magnification. (B) Flow cytometry analysis of CD90.1, CD29, CD45, and CD31 expression. white bar = 200 µm

Flow cytometry analysis was performed to validate MSC surface markers, demonstrating high expression of CD90 (99.50%) and CD29 (96.10%) and low expression of CD45 (1.30%) and CD31 (6.60%) (Figure 1B). Furthermore, the MSCs were evaluated for their ability to differentiate into mature cells. Osteogenic and adipogenic differentiation was induced using specific differentiation media. Osteogenesis was confirmed by calcium deposits stained red with Alizarin Red, and adipogenesis was verified by lipid accumulation stained red with Oil Red O (Figures 3A and B).

The MSCs were incubated under hypoxic conditions (5% O_2 concentration) for 24 hours using a hypoxia chamber. The secretome-containing culture media was collected and filtered using tangential flow filtration (TFF), isolating molecules between 10 and 500 kDa that contained exosomes.

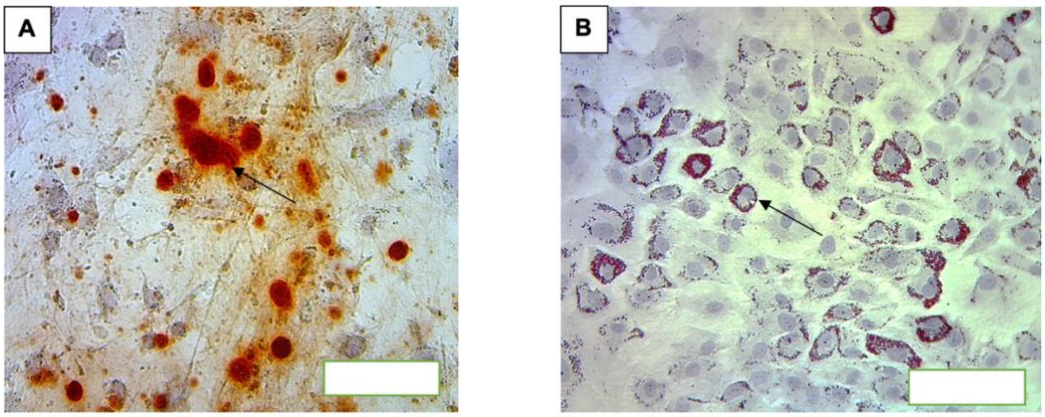

Figure 3. (A) MSCs differentiate into osteocytes and (B) adipocytes after staining with Alizarin Red and Oil Red O at 100x magnification (indicated by black arrows). white bar = 200 µm

Validation of Collagen Loss

This study evaluated the effects of subcutaneous EH-MSC injections on TNF-α and GPx levels in 30 male Wistar rats with UV-B-induced collagen loss. Collagen loss was induced by exposing rats to UV-B radiation at a distance of 20 cm. The exposure intensity was 1 MED (150 mJ/cm²) for 8 minutes, administered 10 times over 14 days. Macroscopic validation was performed by observing wrinkles, which were more prominent in UV-B-exposed rats compared to non-exposed controls (Figure 3).

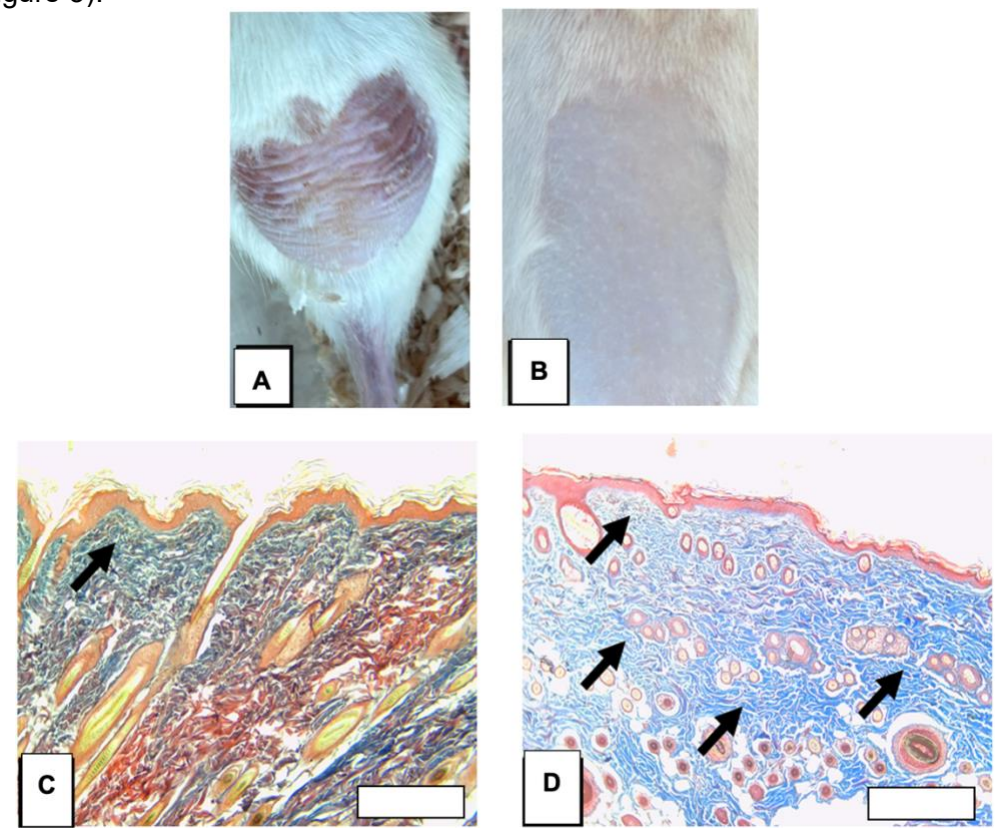

Figure 4. Validation of Collagen Loss.
Wrinkles are more prominent in UV-B exposed rats (A) compared to non-exposed rats (B). Collagen, indicated by blue staining (black arrow), is less visible in the UV-B exposed group (C) compared to the non-UV-B exposed group (D). white bar = 200 µm

Microscopic validation was conducted using Masson's Trichrome staining to assess collagen density in UV-B-exposed skin. Results showed a reduction in

collagen density after UV-B exposure, as indicated by the lower presence of blue-stained collagen fibers in UV-B-exposed samples (Figure 4).

Non-UV-B-exposed rats were classified as the healthy control group (G1). Rats with UV-B-induced collagen loss were divided into four treatment groups: G2 (UV-B + subcutaneous injection of 200 µL 0.9% sodium chloride), G3 (UV-B + subcutaneous injection of 200 µL hyaluronic acid), G4 (UV-B + subcutaneous injection of 200 µL EH-MSC), and G5 (UV-B + subcutaneous injection of 300 µL EH-MSC).

EH-MSC injections were administered once, and skin tissue samples were collected 15 days post-injection. Tissue homogenization was performed using RIPA buffer with protease inhibitors. The supernatant obtained from centrifugation was analyzed for TNF-α and GPx levels using ELISA.

TNF-α and GPx Levels

The TNF-α and GPx levels are summarized in Table 1. The Shapiro-Wilk test showed that TNF-α levels were normally distributed ($p > 0.05$), while GPx levels were not ($p < 0.05$). Levene's test indicated non-homogeneous variance for both TNF-α and GPx ($p < 0.05$). Therefore, parametric (One-Way ANOVA with Tukey Post Hoc) and non-parametric (Kruskal-Wallis with Mann-Whitney) tests were used for TNF-α and GPx data, respectively.

Table 1. TNF-α and GPx Levels in UVB-Induced Skin Damage Rats

Group	TNF-α (pg/mL), Mean ± SD	GPx (pg/mL), Mean ± SD
G1 (Healthy control)	72.08 ± 18.30	52.13 ± 37.73
G2 (NaCl)	208.84 ± 53.80	46.90 ± 11.29
G3 (Hyaluronic acid)	216.80 ± 56.27	145.04 ± 26.57
G4 (EH-MSC Exosomes 200 µL)	122.68 ± 18.95	313.90 ± 101.39
G5 (EH-MSC Exosomes 300 µL)	107.97 ± 24.06	722.40 ± 57.67
Normality test (Shapiro–Wilk)	$p > 0.05$	$p < 0.05$
Homogeneity test (Levene's)	$p = 0.045$	$p = 0.010$
Overall comparison	One-way ANOVA, $p < 0.001$	Kruskal–Wallis, $p < 0.001$

The G1 group had the lowest TNF-α levels (72.08 ± 18.30 pg/mL), followed by G5 (107.97 ± 24.06 pg/mL), G4 (122.68 ± 18.95 pg/mL), and G2 (208.84 ± 53.80 pg/mL), while G3 had the highest levels (216.80 ± 56.27 pg/mL). Subcutaneous EH-MSC injections at both 200 µL and 300 µL doses significantly reduced TNF-α levels compared to the G2 group. For GPx, the highest levels were observed in the G5 group (722.40 ± 57.67 pg/mL), followed by G4 (313.90 ± 101.39 pg/mL), G3 (145.04 ± 26.57 pg/mL), G1 (52.13 ± 37.73 pg/mL), and G2 (46.90 ± 11.29 pg/mL). GPx levels significantly increased in the EH-MSC-treated groups (G4 and G5) compared to the G2 group. The research data show that the highest GPx levels were recorded in G5, with an average value of (722.60 ± 57.67 pg/mL). Conversely, the group with the lowest GPx levels was G2, with an average value of (46.90 ± 11.29 pg/mL). In sequential order, G1 exhibited an average level of (52.13 ± 37.73 pg/mL), followed by G3 with an average level of (145.04 ± 26.57 pg/mL), and then G4 with an average level of (313.90 ± 101.39 pg/mL). Thus, there were significant variations in GPx levels between the groups.

Based on the analysis in Table 1, which revealed significant disparities in TNF-α and GPx levels among treatment groups, post hoc pairwise comparisons were conducted to ascertain specific intergroup differences (Table 2). The Post Hoc Tukey analysis indicated that the healthy control group (G1) exhibited significantly reduced TNF-α levels in contrast to both the NaCl-treated group (G2) and the hyaluronic acid group (G3) ($p < 0.001$ for both comparisons). Nonetheless, no substantial changes were seen between G1 and the EH-MSC exosome-treated groups (G4 and G5) ($p > 0.05$), suggesting that exosome treatment effectively normalized TNF-α levels.

Subsequent comparisons revealed no significant change between G2 and G3 (p = 0.997), indicating that hyaluronic acid did not substantially mitigate UVB-induced inflammation. Conversely, both groups treated with EH-MSC exosomes (G4 and G5) demonstrated markedly reduced TNF-α levels in comparison to G2 (p = 0.015 and p = 0.004, respectively) and G3 (p = 0.007 and p = 0.002, respectively). No substantial difference was observed between G4 and G5 (p = 0.972), suggesting analogous anti-inflammatory effects across the two exosome dosages.

The Mann–Whitney U test revealed significant differences in GPx levels across the majority of pairwise comparisons. In comparison to the healthy control group (G1), GPx levels were markedly elevated in G3, G4, and G5 ($p < 0.05$), although no significant change was noted between G1 and G2 (p = 0.465). Moreover, GPx levels in both EH-MSC exosome-treated groups (G4 and G5) were markedly elevated compared to the NaCl (G2) and hyaluronic acid (G3) groups ($p < 0.05$ for all comparisons). A notable difference was seen between G4 and G5 (p = 0.009), indicating a dose-dependent enhancement in antioxidant activity.

Table 2. Pairwise Comparisons of TNF-α and GPx Levels Between Groups

Group	Comparison Group	TNF-α (Tukey test) (p-value)	GPx (Mann–Whitney test) (p-value)
G1	G2	< 0.001	0.465
	G3	< 0.001	0.016
	G4	0.263	0.009
	G5	0.585	0.009
G2	G3	0.997	0.009
	G4	0.015	0.009
	G5	0.004	0.009
G3	G4	0.007	0.028
	G5	0.002	0.009
G4	G5	0.972	0.009

In accordance with the results shown in Table 1, which indicated increased TNF-α and decreased GPx levels in UVB-exposed rats, the post hoc analysis further substantiates that subcutaneous delivery of EH-MSC-derived exosomes significantly influences both inflammatory and oxidative stress indicators. The absence of notable disparities in TNF-α levels between the exosome-treated groups and the healthy control group suggests that EH-MSC exosomes proficiently mitigate UVB-induced inflammatory responses, presumably via immunomodulatory pathways.

The hyaluronic acid therapy did not substantially vary from saline in its effect on lowering TNF-α levels, indicating limited anti-inflammatory activity under the experimental conditions. The significant increase in GPx levels in exosome-treated groups, especially at the elevated dosage, signifies improved antioxidant defense against oxidative stress. The documented dose-dependent elevation in GPx further corroborates the function of EH-MSC exosomes in stimulating intrinsic antioxidant mechanisms.

Collectively, these findings reinforce the evidence that exosomes produced from EH-MSCs provide dual protective benefits by mitigating inflammation and augmenting antioxidant capacity in UVB-induced skin injury. This integrative impact may aid in maintaining skin structural integrity and underscores the therapeutic potential of EH-MSC exosomes as a cell-free intervention for UVB-induced skin damage.

As summarized in Table 1, UVB exposure markedly increased TNF-α levels and reduced GPx activity in the saline-treated group, indicating the presence of persistent inflammation and oxidative stress. These quantitative findings were further visualized in Figure 4, which illustrates the effects of EH-MSC–derived exosome administration on inflammatory and antioxidant markers. Figure 4A shows that TNF-α levels were substantially elevated in the NaCl (G2) and

hyaluronic acid (G3) groups compared with the healthy control (G1), consistent with the numerical data presented in Table 1. In contrast, subcutaneous administration of EH-MSC exosomes at doses of 200 µL (G4) and 300 µL (G5) markedly reduced TNF-α levels. These reductions were statistically significant when compared with G2 and G3, in accordance with the post hoc Tukey analysis reported in Table 2, while no significant differences were observed between the exosome-treated groups and the healthy control. Figure 4B demonstrates a progressive increase in GPx levels across the treatment groups. As previously shown in Table 1, GPx levels were lowest in the saline group (G2) and increased following hyaluronic acid treatment (G3). Notably, EH-MSC exosome administration resulted in a pronounced elevation of GPx levels in G4 and G5, with the highest levels observed at the 300 µL dose. These differences were statistically significant based on Mann–Whitney post hoc comparisons (Table 2), confirming a dose-dependent enhancement of antioxidant capacity.

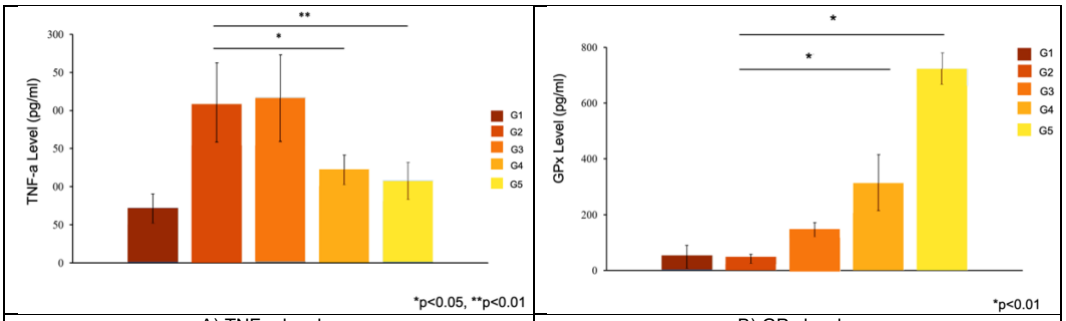

A) TNF-α levels. B) GPx levels.

*Data are presented as mean ± SD. TNF-α was analyzed using one-way ANOVA followed by Tukey post hoc test, while GPx was analyzed using Kruskal–Wallis followed by Mann–Whitney U test. *p < 0.05, **p < 0.01*

Figure 4. Effects of EH-MSC–derived exosomes on inflammatory and oxidative stress markers in UVB-exposed rats.

Figure 4 visually confirms and complements the tabular results by distinctly demonstrating the dual modulatory effects of EH-MSC-derived exosomes on inflammation and oxidative stress in UVB-induced skin damage. The significant decrease in TNF-α levels in the exosome-treated groups indicates successful attenuation of UVB-induced inflammatory responses, aligning cytokine levels more closely with those found in healthy skin. This discovery aligns with the immunomodulatory characteristics of MSC-derived exosomes, recognized for their role in regulating pro-inflammatory cytokine signaling.

The dose-dependent rise in GPx levels concurrently underscores the ability of EH-MSC exosomes to augment intrinsic antioxidant defenses. The markedly elevated GPx levels reported in the high-dose exosome group indicate a potential adaptive mechanism that could safeguard skin tissue from oxidative injury caused by UVB radiation. Collectively, our findings suggest that EH-MSC-derived exosomes provide a synergistic protective impact by reducing inflammation and enhancing antioxidant processes. Integrating the quantitative data from Tables 1 and 2 with the visual patterns in Figure 4 yields persuasive evidence that EH-MSC exosomes present a multimodal, cell-free therapeutic approach for alleviating UVB-induced skin damage.

This study aimed to evaluate the impact of EH-MSC injections at different doses (200 µL and 300 µL) on male Wistar rats exposed to repeated UVB radiation over two weeks. The findings demonstrated that subcutaneous injections of EH-MSC at both doses successfully reduced TNF-α levels. Additionally, the injections at 200 µL and 300 µL also increased GPx levels. This indicates the potential of subcutaneous EH-MSC injections as effective anti-inflammatory and antioxidant agents for UVB-exposed skin [7,12].

The process of photoaging involves complex skin responses to UV radiation, resulting in significant structural and molecular changes. UVB exposure triggers DNA damage, increases ROS production, induces oxidative stress, and stimulates collagen loss, leading to premature skin aging [1,31]. UVB exposure also activates the NF-κB signaling pathway in the skin, which results in the production of pro-inflammatory cytokines, including TNF-α [32,33].

The study found that the group exposed to UVB and treated subcutaneously with hyaluronic acid had the highest TNF-α levels among all groups. This suggests prolonged inflammation in the skin area after UVB exposure. The study also revealed that subcutaneous injections of EH-MSC at doses of 200 µL and 300 µL significantly reduced TNF-α levels, demonstrating the anti-inflammatory activity of EH-MSC injections [7].

EH-MSCs contain various types of miRNAs and cytokines that play critical roles in alleviating inflammation. miR-146a, miR-155, and miR-21 have been identified as key regulators in controlling inflammatory responses.[10] miR-146a and miR-155 suppress TNF-α expression and regulate the NF-κB pathway, while miR-21 is involved in reducing oxidative stress.[34] This is important because NF-κB activation is associated with the production of pro-inflammatory cytokines such as TNF-α, which contribute to skin inflammation and immune responses.

Recent studies indicate that TNF-α expression suppresses GPx activity, while prolonged UVB-induced inflammation reduces GPx levels, increasing ROS and oxidative stress. However, miR-21 in EH-MSC restores GPx levels, neutralizing ROS and reducing oxidative stress.[12] By regulating the NF-κB pathway, EH-MSCs decrease TNF-α and increase GPx, functioning as antioxidants in the inflammatory response to UVB exposure.

Study by Gao et al. (2021) demonstrated that exosomes derived from adipose-derived stem cells (ADSCs) mitigate UVB-induced photoaging in human dermal fibroblasts by reducing intracellular ROS, DNA damage, and MMP-1 expression through regulation of the Nrf2 and MAPK/AP-1 pathways, while also activating the TGF-β/Smad pathway to enhance procollagen type I expression. [13] Similarly in this studies highlight the role of exosomes in combating oxidative stress and supporting collagen synthesis, with EH-MSCs additionally showing anti-inflammatory effects via NF-κB pathway regulation.

Similarly, Yan et al. (2023) reported that bone marrow-derived MSC exosomes containing miR-29b-3p alleviate UVB-induced photoaging by suppressing matrix metalloproteinases (MMPs) in vitro (36). Like our study, Yan et al. utilized MSC-derived exosomes in a UVB-induced model to target inflammatory and oxidative pathways, demonstrating their potential in mitigating photoaging-related damage. However, while Yan et al.'s in vitro study focused on MMP suppression, our in vivo findings emphasize EH-MSC's dual role in reducing TNF-α and increasing GPx in UVB-exposed rats, offering a broader therapeutic impact on both inflammatory and oxidative pathways in skin damage.

Previous research shows MSC secretomes suppress inflammation by reducing TNF-α and stimulating antioxidant proteins like GPx, which combat free radicals. This aligns with the current findings of reduced TNF-α levels and increased GPx levels after EH-MSC treatment in UVB-exposed skin.

[712]Although subcutaneous EH-MSC injections reduced TNF-α and increased GPx via the NF-κB pathway, the precise mechanisms remain unclear. [7] The study did not identify specific miRNAs responsible for these effects, leaving the pathways underlying TNF-α suppression and GPx elevation unexplored [12]. Additionally, limitations include the small sample size may limit statistical power, the lack of long-term follow-up to assess sustained effects, and the absence of further histopathological or molecular analyses to elucidate tissue-level changes. These limitations highlight the need for further research to validate and expand these findings.

CONCLUSION

Subcutaneous administration of EH-MSC–derived exosomes effectively attenuated inflammatory responses and enhanced antioxidant activity in UVB-exposed Wistar rats, as evidenced by a significant reduction in TNF-α levels and a concomitant increase in GPx levels. Rats treated with EH-MSC exosomes at doses of 200 µL (G4) and 300 µL (G5) exhibited significantly improved inflammatory and oxidative stress profiles compared with the saline-treated control group. Moreover, the higher exosome dose produced a more pronounced enhancement of GPx activity, indicating a dose-dependent modulation of oxidative stress responses. Collectively, these findings support the therapeutic potential of EH-MSC–derived exosomes as a cell-free approach for mitigating UVB-induced skin inflammation and oxidative damage. Future studies should investigate the molecular mechanisms underlying the anti-inflammatory and antioxidant effects of EH-MSC–derived exosomes, including the role of exosomal microRNAs and signaling pathways involved in redox regulation. Long-term and dose-optimization studies are also warranted to assess the durability and safety of EH-MSC exosome therapy. In addition, evaluating the effects of EH-MSC exosomes on structural and functional skin parameters, such as collagen synthesis, histopathological changes, and barrier function, will be essential to establish their translational relevance. Ultimately, well-designed preclinical and clinical studies are needed to confirm the efficacy and safety of EH-MSC–derived exosomes for potential therapeutic application in UVB-related skin disorders.

AUTHORS' CONTRIBUTIONS

M, AP, C, and ES were involved in concepting and planning the research; M performed the data acquisition/collection, calculated the experimental data, performed the data, drafted the manuscript and designed the figures, and interpreting the results. All authors took parts in giving critical revision of the manuscript.

FUNDING INFORMATION

There is no funding source.

DATA AVAILABILITY STATEMENT

The datasets generated and analyzed during the current study are available from the corresponding author upon reasonable request.

REFERENCES

1. Pourang A, Tisack A, Ezekwe N, et al. Effects of visible light on mechanisms of skin photoaging. *Photodermatol Photoimmunol Photomed*. 2022;38(3):191-196. doi:10.1111/phpp.12736
2. Yang YN, Wang F, Zhou W, Wu ZQ, Xing YQ. TNF-α Stimulates MMP-2 and MMP-9 Activities in Human Corneal Epithelial Cells via the Activation of FAK/ERK Signaling. *Ophthalmic Res*. 2012;48(4):165-170. doi:10.1159/000338819
3. Mirastschijski U, Lupše B, Maedler K, et al. Matrix Metalloproteinase-3 is Key Effector of TNF-α-Induced Collagen Degradation in Skin. *Int J Mol Sci*. 2019;20(20). doi:10.3390/ijms20205234
4. Chircov C, Grumezescu AM, Bejenaru LE. Hyaluronic acid-based scaffolds for tissue engineering. *Rom J Morphol Embryol*. 2018;59(1):71-76.
5. Nejati S, Mongeau L. Injectable, pore-forming, self-healing, and adhesive hyaluronan hydrogels for soft tissue engineering applications. *Sci Rep*. 2023;13(1):14303. doi:10.1038/s41598-023-41468-9
6. Trong HN, Phuong TVT, Van TN, et al. The Efficacy and Safety of Hyaluronic Acid Microinjection for Skin Rejuvenation in Vietnam. *Open*

Access Maced J Med Sci. 2019;7(2):234-236. doi:10.3889/oamjms.2019.059
7. Ha DH, Kim H keun, Lee J, et al. Mesenchymal Stem/Stromal Cell-Derived Exosomes for Immunomodulatory Therapeutics and Skin Regeneration. *Cells*. 2020;9(5):1157. doi:10.3390/cells9051157
8. Nath Neerukonda S, Egan NA, Patria J, et al. Comparison of exosomes purified via ultracentrifugation (UC) and Total Exosome Isolation (TEI) reagent from the serum of Marek's disease virus (MDV)-vaccinated and tumor-bearing chickens. *J Virol Methods*. 2019;263:1-9. doi:10.1016/j.jviromet.2018.10.004
9. Zabaglia LM, Sallas ML, Santos MP Dos, et al. Expression of miRNA-146a, miRNA-155, IL-2, and TNF-α in inflammatory response to Helicobacter pylori infection associated with cancer progression. *Ann Hum Genet*. 2018;82(3):135-142. doi:10.1111/ahg.12234
10. Cai G, Cai G, Zhou H, et al. Mesenchymal stem cell-derived exosome miR-542-3p suppresses inflammation and prevents cerebral infarction. *Stem Cell Res Ther*. 2021;12(1):2. doi:10.1186/s13287-020-02030-w
11. Li X, Liu L, Yang J, et al. Exosome Derived From Human Umbilical Cord Mesenchymal Stem Cell Mediates MiR-181c Attenuating Burn-induced Excessive Inflammation. *EBioMedicine*. 2016;8:72-82. doi:10.1016/j.ebiom.2016.04.030
12. Norouzi-Barough L, Shirian S, Gorji A, Sadeghi M. Therapeutic potential of mesenchymal stem cell-derived exosomes as a cell-free therapy approach for the treatment of skin, bone, and cartilage defects. *Connect Tissue Res*. 2022;63(2):83-96. doi:10.1080/03008207.2021.1887855
13. Gao W, Wang X, Si Y, et al. Exosome Derived from ADSCs Attenuates Ultraviolet B-mediated Photoaging in Human Dermal Fibroblasts. *Photochem Photobiol*. 2021;97(4):795-804. doi:10.1111/php.13370
14. Putra A, Alif I, Hamra N, et al. MSC-released TGF-β regulate α-SMA expression of myofibroblast during wound healing. *J Stem Cells Regen Med*. 2020;16(2):73-79. doi:10.46582/jsrm.1602011
15. Yan T, Huang L, Yan Y, Zhong Y, Xie H, Wang X. Bone marrow mesenchymal stem cell-derived exosome <scp>miR</scp> -29b-3p alleviates <scp>UV</scp> irradiation-induced photoaging in skin fibroblast. *Photodermatol Photoimmunol Photomed*. 2023;39(3):235-245. doi:10.1111/phpp.12827
16. Guan L, Suggs A, Galan E, Lam M, Baron E. Topical application of ST266 reduces UV-induced skin damage. *Clin Cosmet Investig Dermatol*. 2017;Volume 10:459-471. doi:10.2147/CCID.S147112
17. Xue Y, Chen L, Li B, et al. Genome-wide mining of gpx gene family provides new insights into cadmium stress responses in common carp (Cyprinus carpio). *Gene*. 2022;821:146291. doi:10.1016/j.gene.2022.146291
18. Tian R, Geng Y, Yang Y, Seim I, Yang G. Oxidative stress drives divergent evolution of the glutathione peroxidase (GPX) gene family in mammals. *Integr Zool*. 2021;16(5):696-711. doi:10.1111/1749-4877.12521
19. Zhou Y, Li J, Wang J, Yang W, Yang Y. Identification and Characterization of the Glutathione Peroxidase (GPX) Gene Family in Watermelon and Its Expression under Various Abiotic Stresses. *Agronomy*. 2018;8(10):206. doi:10.3390/agronomy8100206
20. Pittenger MF, Mackay AM, Beck SC, et al. Multilineage Potential of Adult Human Mesenchymal Stem Cells. *Science (1979)*. 1999;284(5411):143-147. doi:10.1126/science.284.5411.143
21. Bieback K, Hecker A, Kocaömer A, et al. Human Alternatives to Fetal Bovine Serum for the Expansion of Mesenchymal Stromal Cells from Bone Marrow. *Stem Cells*. 2009;27(9):2331-2341. doi:10.1002/stem.139

22. Alwohoush E, Ismail MA, Al-Kurdi B, et al. Effect of hypoxia on proliferation and differentiation of induced pluripotent stem cell-derived mesenchymal stem cells. *Heliyon*. 2024;10(19):e38857. doi:10.1016/j.heliyon.2024.e38857
23. Théry C, Witwer KW, Aikawa E, et al. Minimal information for studies of extracellular vesicles 2018 (MISEV2018): a position statement of the International Society for Extracellular Vesicles and update of the MISEV2014 guidelines. *J Extracell Vesicles*. 2018;7(1). doi:10.1080/20013078.2018.1535750
24. Gu Y, Han J, Jiang C, Zhang Y. Biomarkers, oxidative stress and autophagy in skin aging. *Ageing Res Rev*. 2020;59:101036. doi:10.1016/j.arr.2020.101036
25. Angelina J, Putra A, Trisnadi S, et al. Hypoxia-conditioned mesenchymal stem cells (MSC) exosomes attenuate ultraviolet-B (UVB)-mediated malondialdehyde (MDA) and matrix metalloproteinase-1 (MMP)-1 upregulation in collagen loss models. *Med Glas*. 2025;22(1):9-14. doi:10.17392/1923-22-01
26. Wlaschek M, Tantcheva-Poór I, Naderi L, et al. Solar UV irradiation and dermal photoaging. *J Photochem Photobiol B*. 2001;63(1-3):41-51. doi:10.1016/S1011-1344(01)00201-9
27. Fischer AH, Jacobson KA, Rose J, Zeller R. Hematoxylin and Eosin Staining of Tissue and Cell Sections. *Cold Spring Harb Protoc*. 2008;2008(5):pdb.prot4986. doi:10.1101/pdb.prot4986
28. Witwer KW, Buzás EI, Bemis LT, et al. Standardization of sample collection, isolation and analysis methods in extracellular vesicle research. *J Extracell Vesicles*. 2013;2(1). doi:10.3402/jev.v2i0.20360
29. Crowther JR. *The ELISA Guidebook*. Vol 516. Humana Press; 2009. doi:10.1007/978-1-60327-254-4
30. SPSS Statistics. Accessed September 29, 2025. https://www.ibm.com/mysupport/s/topic/0TO500000001yjtGAA/spss-statistics?language=en_US
31. Shah K, Minkis K, Swary JH, Alam M. Photoaging. In: *Cosmetic Dermatology*. Wiley; 2022:16-25. doi:10.1002/9781119676881.ch2
32. Chandel NS, Trzyna WC, McClintock DS, Schumacker PT. Role of Oxidants in NF-κB Activation and TNF-α Gene Transcription Induced by Hypoxia and Endotoxin. *The Journal of Immunology*. 2000;165(2):1013-1021. doi:10.4049/jimmunol.165.2.1013
33. Bashir MM, Sharma MR, Werth VP. UVB and proinflammatory cytokines synergistically activate TNF-alpha production in keratinocytes through enhanced gene transcription. *J Invest Dermatol*. 2009;129(4):994-1001. doi:10.1038/jid.2008.332
34. De Freitas JH, Bragato JP, Rebech GT, et al. MicroRNA-21 and microRNA-148a affects PTEN, NO and ROS in canine leishmaniasis. *Front Genet*. 2023;14:1106496. doi:10.3389/fgene.2023.1106496